University of New Hampshire
University of New Hampshire Scholars' Repository

Honors Theses and Capstones

Student Scholarship

Spring 2016

Physical Modeling of the Atmospheric Boundary Layer in the University of New Hampshire's Flow Physics Facility

Stephanie Gilooly
University of New Hampshire, sem748@wildcats.unh.edu

Gregory Taylor-Power
University of New Hampshire, gga3@wildcats.unh.edu

Follow this and additional works at: https://scholars.unh.edu/honors

Part of the Mechanical Engineering Commons, and the Other Engineering Commons

Recommended Citation

Physical Modeling of the Atmospheric Boundary Layer in the University of New Hampshire's Flow Physics Facility

Stephanie Gilooly and Gregory Taylor-Power
Advisors: Dr. Joseph Klewicki, Dr. Martin Wosnik, John Turner V

ME 755 Final Report
May 10, 2016

I. Abstract

The atmospheric boundary layer is the lowest part of the atmosphere, and is defined by a region from the surface of the earth to approximately 500-1000m altitude in which air velocity changes from zero at the surface to a faster free stream velocity at a high altitude. This region of the atmosphere is of interest because it affects everyday life, from constructing a tall building to airplane travel and kite flying. The energy from the wind can also be harvested into electricity through wind turbines. The type of atmospheric boundary layer is characterized by the terrain it encounters, varying from open sea and mud flats to suburban areas and city centers with high- and low-rise buildings. The goal of this project is to generate rescaled versions of different types of atmospheric boundary layers for scale model testing in the UNH Flow Physics Facility (FPF).

The project began with the analysis of smooth wall (baseline) data previously recorded in the FPF. Several arrays of roughness elements were designed to simulate varying roughness lengths experienced by atmospheric boundary layers and were tested in the FPF. The resulting velocity profiles in the boundary layer were measured using hot wire anemometry and pitot static tubes. These measured velocity profiles (mean and fluctuating) and velocity spectra were compared to atmospheric boundary layers using ASCE Standards (ASCE/SEI 49-12) [1]. This application can then be used in the future for wind engineering studies, such as the structural analysis of buildings.

II. Introduction and Research Objectives

This report analyzes the effect of roughness elements on the velocity profile in the UNH Flow Physics Facility (FPF) boundary layer wind tunnel. These roughness elements are added for the purpose of simulating the suburban atmospheric boundary layer. Suburban terrains were the initial goal of the project as building analyses could be performed in this category. The FPF is a large boundary layer wind tunnel with dimensions of L=72m, H=2.7m, and W=6m and can be seen in the images below.
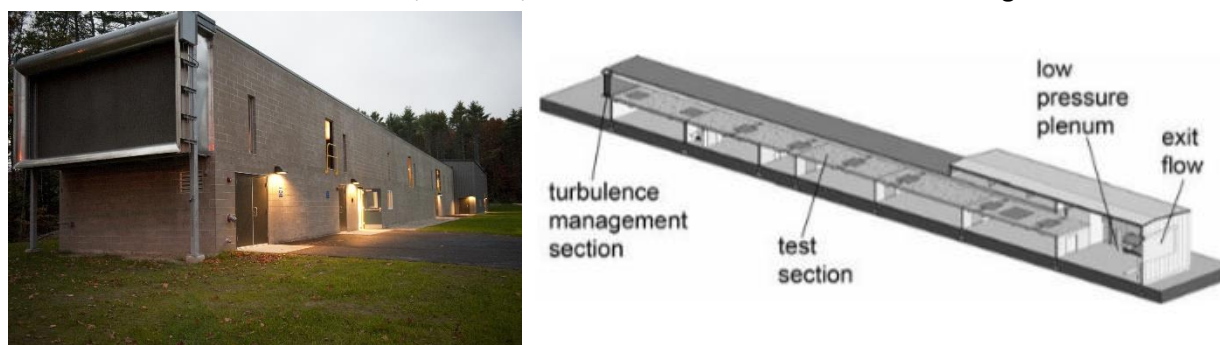

Figure 1: Exterior [5] and Interior [6] of the UNH Flow Physics Facility (FPF). The flow begins at the left of both images and flows to the right and exits through the fans running at a specified rate

The FPF was designed to study large-scale high Reynolds number turbulent boundary layers. Its large size also gives it great potential for wind energy and wind engineering studies. The first step in performing these studies is creating a good simulation of the atmospheric boundary layer.

To use the FPF for wind engineering studies, one must be able to recreate scaled-down versions of atmospheric boundary layers. The atmospheric boundary layer, or ABL, is the region of air flowing over Earth's surface that is affected by the surface. Any structures that need to undergo wind studies, such as buildings and wind turbines, exist in the ABL. Simulating the ABL in a wind tunnel ensures that any structures in wind energy or wind engineering experiments performed will be subjected to a similar wind profile to the full scale. The ABL varies with the different terrains of the Earth's surface, so the FPF needs to reproduce many different boundary layers with ABL parameters specified by the American Society of Civil Engineers (ASCE). [1] Figure 2 below demonstrates how the boundary layer height and profile shape vary with varying terrain. The urban terrain on the left disturbs the flow the most and the ocean sea on the right disturbs the flow the least.
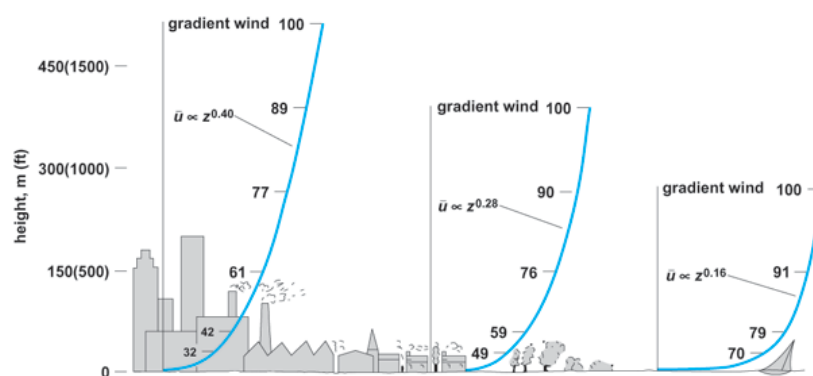
Figure 2: ABL Profiles varying terrain. The mean wind speed, u, represented as a percent of the freestream velocity is plotted versus height, z for the wind within the boundary layer. [4]

The main objective of this project is to generate different types of scale models of the ABL for testing in the FPF. These models are developed through the design and construction of various roughness elements. The resulting boundary layer properties will then be measured and compared to the existing ASCE standards.

III. Theory of Boundary Layers

A boundary layer forms when a viscous flow interacts with another surface. The boundary layer is the region of flow that is affected by this interaction, or the layer of fluid near the surface where there is a velocity gradient. The constant velocity outside this region is known as the freestream velocity. The flow at surface is defined by the no slip condition, meaning that the velocity of the fluid is the same as the velocity of the surface. For example, if the fluid is moving over a stationary solid surface, the velocity of the flow is zero at the surface. At the top of the boundary layer, the velocity remains the freestream velocity, U_∞. Between these points, the flow velocity varies like in Figure 3. The shape of the velocity profile between these points varies for different flows. The boundary layer height, δ, is usually defined as the position corresponding to a velocity value that is 99% of the freestream velocity. Figure 3 demonstrates the physical meaning of these parameters. [3]
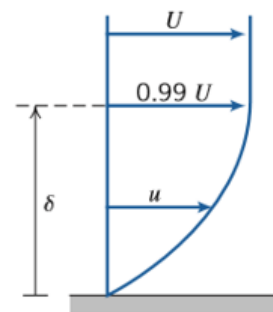
Figure 3: Physical demonstration of freestream velocity and boundary layer height on a velocity profile [3]

The shape of this profile has steeper velocity gradients near the wall if the flow is turbulent as opposed to laminar. Laminar flow has a low Reynolds number and does not have as much momentum convection as turbulent flow. A turbulent boundary layer occurs in higher Reynolds number flows due to the imbalance of momentum between flow inside and outside of the boundary layer. This study recreates scaled-down versions of the turbulent boundary layers created by the wind interacting with Earth's surface, henceforth called atmospheric boundary layers, or ABLs. The turbulence in atmosphere causes high fluctuations of velocity which are challenging to predict and model numerically.

There are several parameters other than the velocity and boundary layer height that characterize these flows. The air has a density, ρ, and a kinematic viscosity, v, which are properties of the fluid and vary with temperature and humidity. Another property is the roughness length, y_o, which is one of the parameters specified in the ASCE Standards. The roughness length is a length-scale that represents the average roughness of a surface. A smooth surface, like the open sea, has a small roughness length compared to a suburban or urban landscape.

Friction velocity, u_τ, is a shear stress value rewritten in units of velocity, and it is dependent on the slope of the velocity gradient at the wall. It characterizes the shear effects in the flow and is commonly used to normalize parameters close to the wall. To use this normalization is to "inner-normalize," and this involves making the variables be unit-less using smaller-scale parameters, such as the friction velocity and the kinematic viscosity of the fluid. The typical inner-normalized velocity is u/u_τ. Another approach is to

"outer-normalize" the flow, and this involves larger-scale parameters, such as the freestream velocity and boundary layer height. The typical outer-normalized velocity is u/U_∞, where U_∞ is the freestream velocity. Both of these normalization methods must be used in this project. [3]

IV. Experimental Methods

Before new experiments were performed with added roughness, data previously taken in the FPF was analyzed and compared to ASCE standards to assess the FPF's natural ability to simulate the ABL. This velocity profile data was recorded using a hot wire anemometer in the empty test section of the FPF. The methods for comparing mean velocity profiles to ABL conditions are based on the power law exponent, n, and the roughness length, y_0, of each profile. The power law model for the flow is used to calculate the exponent and is of the form:

$$\frac{U}{U_\infty} = C\left(\frac{y}{\delta}\right)^n \tag{1}$$

where U_∞ is the freestream velocity, δ is the boundary layer height, C is a constant, which is normally equal to one, and n is the exponent. This relationship is applied in the logarithmic region of the flow, which varies slightly for each flow. [1] To calculate the power law fit, equation 1 is rewritten as:

$$\ln\left(\frac{U}{U_\infty}\right) = n\ln\left(\frac{y}{\delta}\right) + \ln(C) = A\ln\left(\frac{y}{\delta}\right) + B \tag{2}$$

where A and B are constants that can be found using the "polyfit" function in MATLAB. The best power law fit for each profile was determined quantitatively by calculating the root mean square difference (RMSD) for a range of exponents. The fit with the lowest RMSD was considered the best fit.

A logarithmic distribution can be used to estimate the friction velocity and roughness length of each flow. The logarithmic distribution is characterized by the following equation from [1]:

$$U(y) = (u_\tau/\kappa)\ln(y/y_0) \tag{3}$$

Equation (9) can be rewritten such that a "polyfit" function can be used to find the desired parameters (u_τ and z_o). [1] The rewritten equation is:

$$U(y) = \left(\frac{u_\tau}{\kappa}\right)\ln(y) - \left(\frac{u_\tau}{\kappa}\right)\ln(y_0) = D\ln(y) + E \tag{4}$$

where D and E are constants found in MATLAB. An RMSD method was used again to optimize the log fit.

These methods are used to analyze the characteristics of the mean flow. To analyze the fluctuations of the flow, the power spectral density of the flow must be calculated and compared to the standards. Power spectral density analysis characterizes the distribution of eddy sizes within the flow, and

their kinetic energy content. The energetics of the flow are well-modeled if the theoretical and experimental spectra agree. The normalized experimental spectra is:

$$\frac{f\phi}{\overline{u}^2} \tag{5}$$

where f is the frequency, ϕ is the spectral density, and $\overline{u}^2$ is the root mean square of the velocity. The normalized Von Karman (theoretical) spectra given in the ASCE standard is:

$$\frac{fS_u(y,f)}{\sigma^2} = \frac{4f^x L_u/U}{[1 + 70.8(f^x L_u/U)^2]^{5/6}} \tag{6}$$

where $^x L_u$ is the integral scale of the horizontal component of velocity in the x direction. This theoretical spectra can be compared to the experimental spectra generated from the fluctuating component of the velocity [1]. To determine a region in which the experimental and theoretical spectra are comparable, the RMSD was calculated for each point and a tolerance was set. The tolerances chosen for these regions are discussed in the results.

After the existing data was analyzed, roughness elements were created and the rough wall boundary layer profiles were measured. The boundary layer velocity profiles were measured using both a pitot tube and a hot wire anemometer. The pitot tube was chosen for its ability to measure the mean velocity well, and the hot wire was used to measure high frequency fluctuations in wind velocity. The measurement devices were mounted to a programmable vertical traversing system that was operated via MATLAB. The velocity profiles were all measured at 16m downstream of the FPF test section inlet with the fans set to 600 RPM. This location was chosen so the data could be compared to measurements previously taken in the FPF [6].

The profiles were created by measuring the air velocity at multiple points above the floor. A logarithmic spacing was used to for these points to ensure that the steep velocity gradient near the floor was captured in the data. Each point was measured for 4 minutes at a sampling rate of 10 kHz. The hot wire was calibrated before and after each test using a polynomial fit between 6 calibration speeds. Air density and viscosity were calculated for each test using the corresponding air temperature and humidity.

To generate rough boundary layer flows for the purpose of ABL simulation, an array of roughness was created and placed upstream of the measurement location. The calculations for the roughness elements were taken from Counihan (1971) [2]. The equation that is empirically formulated in this paper is as follows,

$$\frac{y_0}{h} \cong 8.2 \cdot \frac{h}{f} + 1.08 \cdot \frac{A_R}{A} - 0.08 \tag{7}$$

where y_0 is the roughness length, h is the individual roughness element height, f is the roughness array fetch length, A_R is the total surface area of the roughness elements, and A is the total plan surface area of the array [2]. A_R/A is referred to as the roughness element density. When the roughness array fetch length is much larger than the roughness element height, the equation can be approximated to:

$$\frac{y_0}{h} \cong 1.08 \cdot \frac{A_R}{A} - 0.08 \qquad (8)$$

The study states that this equation is valid for roughness element densities of $0.1 < \frac{A_R}{A} < 0.25$. A roughness element density of 0.1 was chosen for this experiment. A suburban ABL was chosen as the model for the roughness array design. The range of roughness heights for a suburban boundary layer is $1\,m < z_o < 2\,m$. From Vincenti et al. (2013) [6], the boundary layer height in the FPF at 66 m downstream is 0.7363 m. Assuming the ABL has a height of about 1km, and a roughness length of 1.5m, the scaled roughness length required for the FPF can be calculated as follows:

$$y_0 = 1.5m \cdot \left(\frac{0.7363\,m}{1000\,m}\right) = .0011\,m \qquad (9)$$

Knowing this value along with the roughness element density, equation 2 can be manipulated to solve for the block height, h.

$$h = \frac{y_0}{1.08 \cdot \frac{A_R}{A} - 0.08} = \frac{.0011m}{1.08 \cdot 0.1 - 0.08} = .0394\,m \qquad (10)$$

The total number of blocks needed is dependent on the fetch length and block size. The blocks were cut from 4x4 pieces of lumber, which have an area of 0.0079m. Knowing the width of the FPF is 6m, the number of blocks per meter could be calculated. To achieve the area density required, 76 blocks per meter were needed [2]. The array design below was used to create the arrays in the experiment.
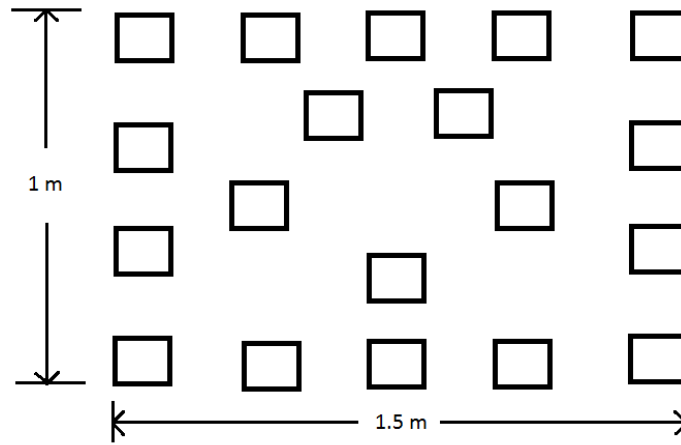
Figure 4: Roughness Array Configuration for a 1.5m x 1m section of the FPF floor. This configuration is then repeated to fill the necessary area, and the columns are staggered to prevent any biased flow.

The analysis techniques used on the Vincenti et al. data were then applied to the new data. Figure 4 shows the configuration used to match the roughness element density required. This pattern was repeated 4 times to cover the width of the FPF, and for however many meters were necessary for the length. After the array was created, the columns were staggered to prevent any bias.

The pitot-static tube outputs a profile of pressure differences measured in torr. To convert this to a velocity profile, Bernoulli's equation for incompressible, inviscid flows, below, is utilized:

$$\frac{P_1}{\rho} + \frac{V_1{}^2}{2} + gz_1 = \frac{P_2}{\rho} + \frac{V_2{}^2}{2} + gz_2 \tag{11}$$

where pressure is in Pa, velocity is in m/s, and position is in m. When applying this to the stagnation point and the static point of the Pitot tube, it is known that the heights are the same, the velocity at the stagnation point is zero and the velocity at the static point is the inlet velocity. Therefore, the equation can be rewritten into something more practical, like this equation below:

$$U = \sqrt{\frac{2(P_{stag} - P_{static})}{\rho_{air}}} \tag{12}$$

The hot wire was calibrated using a 3rd order polynomial fit between 6 calibrations points. To do this, the FPF was run at 6 different fan speeds from 200 RPM to 700 RPM with steps of 100 RPM. The hotwire was placed at the same height as the pitot tube and they recorded data simultaneously. A Matlab "polyfit" command was then used to create a calibration curve for the hotwire data.

V. Experimental Results

Experimental analysis was done for both the existing Vincenti et al. data, and the newly acquired rough wall data. The purpose of this analysis was to compare the characteristics of the boundary layer in the FPF to the ASCE standards for wind tunnel testing. The results of these analyses are shown below.

i. Vincenti et al. Data

Analysis was performed for five Reynolds numbers, but particular attention was paid to the most relevant set of data that was taken at the same location and same speed as the rough wall data. The table below shows the results from all Reynolds numbers analyzed.

Table 1: Results of Vincenti et al. Data Analysis

δ^+	x (m)	Power Law Exponent	U_∞ (m/s)	u_τ (m/s)	δ_{99} (m)	v (m/s^2)	Domains: Spectral Analysis			Domains: Power Law Analysis		
							y (m)	y^+	y/δ	y (m)	y^+	y/δ
1450	4	0.159	6.87	0.263	0.0861	1.562E-05	0.00124-0.0406	21-684	0.01438-0.4717	0-0.0861	0-1450	0-1
2180	8	0.158	6.95	0.252	0.1356	1.568E-05	0.00307-0.0784	49-1261	0.02261-0.5785	0-0.1356	0-2180	0-1
3820	16	0.149	6.87	0.240	0.2456	1.505E-05	0.00607-0.116	97-1851	0.02470-0.4726	0-0.2456	0-3820	0-1
6430	32	0.143	7.01	0.234	0.4284	1.559E-05	0.0095-0.187	104-2812	0.02970-0.8007	0-0.4284	0-6430	0-1
10770	66	0.130	6.95	0.226	0.7363	1.545E-05	0.0243-.435	355-6370	0.0330-0.5914	0-0.7363	0-10770	0-1

It is clear that with increasing Reynolds number, the region in which the power spectral density of the flow matches the theoretical spectra becomes larger. The power law exponent also clearly decreases with Reynolds number, which is expected as the flow becomes more turbulent and the boundary layer flattens.

For the data with Reynolds number $\delta^+ = 3820$ the FPF was run at 600 RPM and the velocity profile was recorded at 16m downstream of the inlet, so it is relevant to the rough data. This profile had a power law exponent of 0.159, which corresponds to a terrain of low crops and occasional large obstacles [1]. Figure 5 shows both a logarithmic and linear plot of this velocity profile with the power law fit overlaid on the data. The power law fits the data very closely from 0.002 m off the floor to the top of the boundary layer. For experimental purposes, this corresponds to the entire boundary layer.
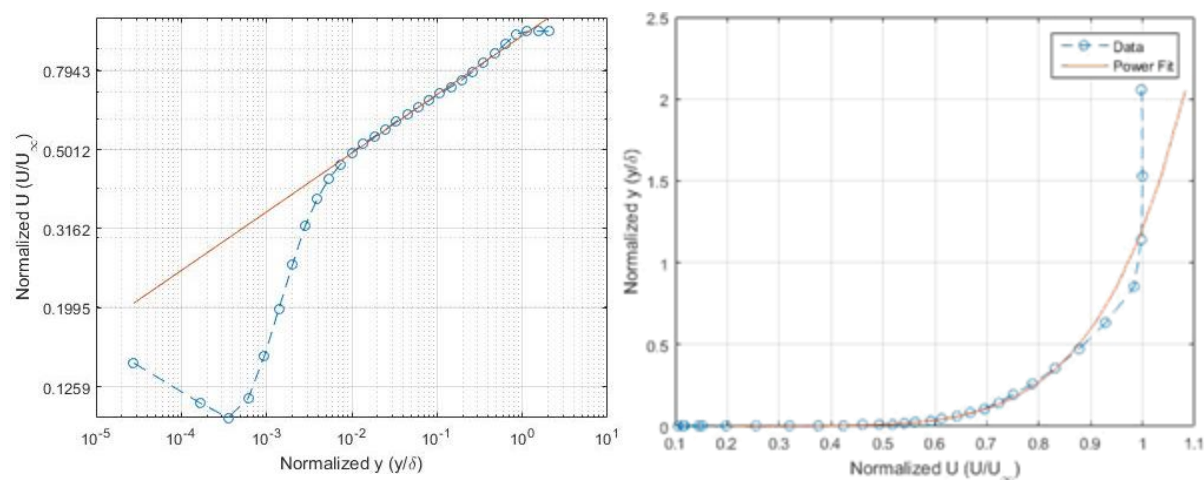
Figure 5: Logarithmic and Linear Plots of mean velocity profiles recorded with a hotwire anemometer at 16m downstream of the FPF inlet with the fans running at 600 RPM. A power law fit with an exponent of n=0.149 is overlaid onto the data

The power spectral density of this data set was comparable for the region of 0.006m to 0.116m off the floor. Figure 6 shows the theoretical and experimental spectra for a point 0.048m off the floor.

The vertical location of this plot is in the middle of the comparable region, and fits very well to the expected spectra. It is expected that the addition of roughness elements will increase the size of the comparable region of spectra.
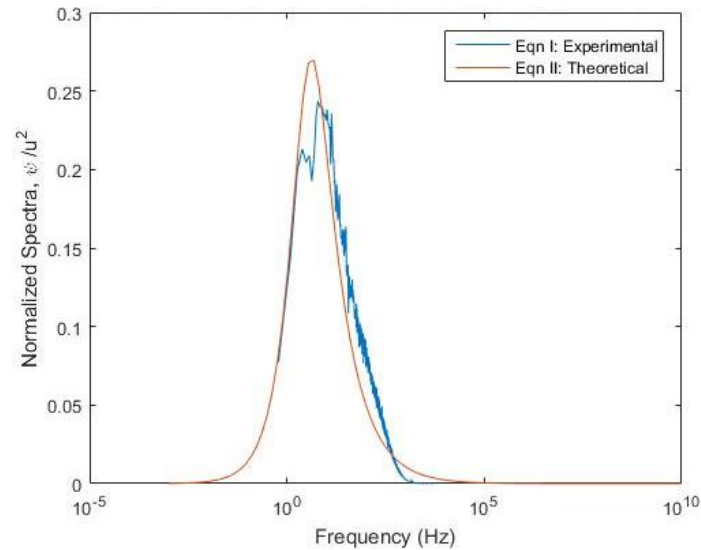
Figure 6: Plot of power spectral density for velocity data taken with a hotwire anemometer at 16m downstream of the FPF inlet at a point .048m above the floor with the fans running at 600 RPM. Theoretical Von Karman Spectra [1] is overlaid

ii. Experimental

Data was collected using a hot wire anemometer and pitot tube for varying fetches in the center of the FPF tunnel, 16 meters downstream from the inlet. Both devices were mounted on a traverse that moved them to precise locations, according to the operator's code. The first experiments had no roughness elements in an attempt to recreate the previous Vincenti data profiles. Then, roughness element fetches of 1 meter, 3 meters, and 6 meters were measured. Figure 7 below was taken when there were 6m of roughness elements in the inlet of the FPF.

Figure 7: Array of Roughness Elements with 6m fetch at the inlet of the FPF. This was the largest array of roughness elements used in these experiments. The traverse used to collect data was 16 m from the inlet of the FPF

A traverse located 16m from the inlet of the tunnel was used to accurately move the pitot tube and hot wire to the desired vertical positions for data collection. The pitot tube experiment outputs the pitot pressure differences in torr, which can be converted to velocity measurements using Bernoulli's equation. The hot wire data is converted to velocity from using a polynomial fit with the pre- and post-calibration data.

The velocity data was then used to calculate the power law exponent such that this parameter can be related to those prescribed in the ASCE standards. The logarithmic plot of outer-normalized velocity versus position can be seen in the figure below. Once again, the straight region to which the power law fit was applied is the logarithmic region of the turbulent flow.
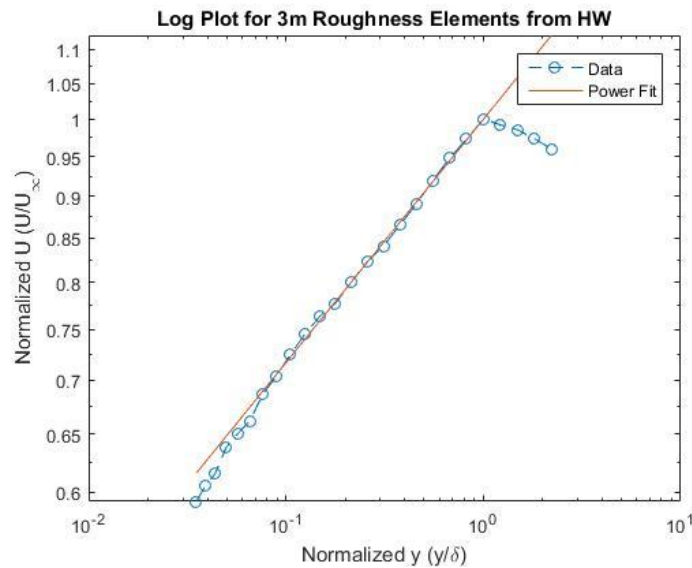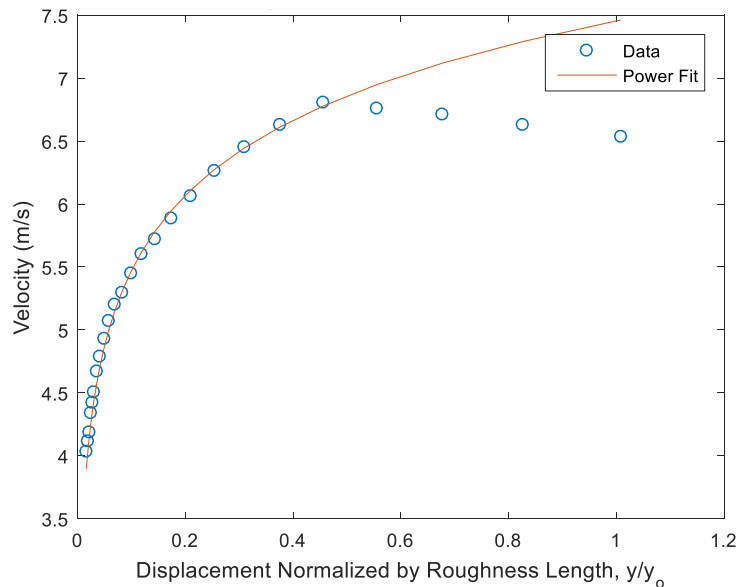

Figure 8: Logarithmic plot of mean velocity profile recorded with a hotwire anemometer at 16m downstream of the FPF inlet with the fans running at 600 RPM with a 3m array of roughness at the inlet. A power law profile with exponent n=0.145 is plotted over the data.

This fit was then plotted on standard axes such that the theoretical and experimental profiles can be more easily compared. Once again, the two profiles are very similar within the boundary layer and outside the boundary layer, the velocity remains roughly constant at the freestream velocity. This is the relationship expected from the power law fit, so the resulting power law exponent should reflect the experimental profile geometry well.
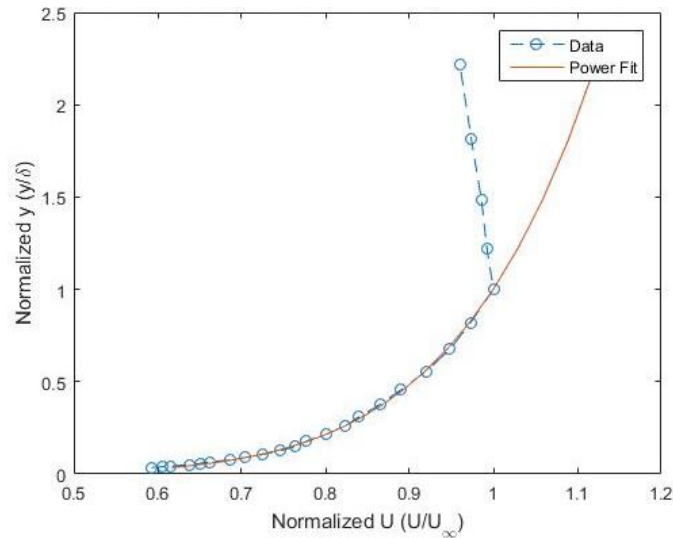
Figure 9: Linear plot of mean velocity profile recorded with a hotwire anemometer at 16m downstream of the FPF inlet with the fans running at 600 RPM with a 3m array of roughness at the inlet. A power law profile with exponent n=0.145 is plotted over the data.

A logarithmic fit was then applied to each data set to determine an estimate of the friction velocity and roughness length of the flow. The figure below demonstrates the logarithmic fit for the data collected with 3m of roughness elements and the hot wire.

Figure 10: Linear plot of mean velocity profile recorded with a hotwire anemometer at 16m downstream of the FPF inlet with the fans running at 600 RPM with a 3m array of roughness at the inlet. A log law estimate with u_τ=0.25m/s and y_0=1.7E-04m is plotted over the data

Again, the theoretical and experimental curves in this figure are closely related until the freestream velocity is reached. Next, the power density spectra was calculated at each position in each

data set to find the domains over which the kinetic energy distributions are comparable to ABL standards. The figure below is the point of best correlation for the 3m hot wire data, although a wide range of points for each data set were comparable.
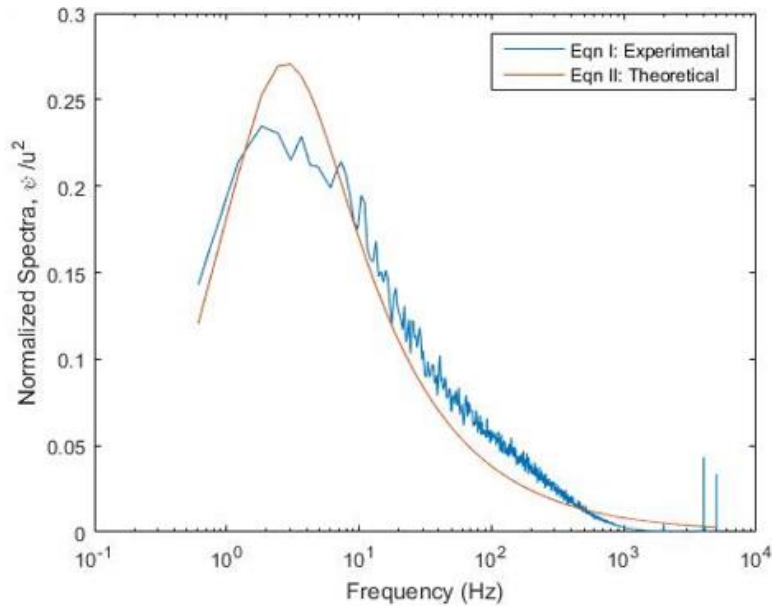
Figure 11: Pre-multiplied power spectral density for velocity data taken with a hot wire anemometer at 16m downstream of the FPF inlet with 3m of roughness array placed at the inlet with the fans running at 600 RPM. The theoretical Von Karman spectra [1] is plotted over the data.

The table below repots the calculated values from this data analysis for each experiment and the regions over which the flow is comparable, according to the theories used thus far.

Table 2: Results of Experimental Data Analysis

	Roughness Element Fetch Length	Power Law Exponent	U_∞ (m/s)	u_τ (m/s)	δ_{99} (m)	y_0 (m)	Domains: Spectral Analysis			Domains: Power Law Analysis		
							y (m)	y^+	y/δ	y (m)	y^+	y/δ
Hot Wire	0 m (smooth)	0.174	6.94	0.36	0.24	3.44E-04	0.021-0.087	526-2205	0.089-0.37	0-0.24	0-5936	0-1
	1 meter	0.124	6.77	0.32	0.37	4.55E-05	0.018-0.19	405-4164	0.049-0.50	0-0.37	0-8341	0-1
	3 meter	0.145	6.44	0.25	0.46	1.74E-04	0.020-0.21	345-3599	0.044-0.46	0-0.46	0-7877	0-1
	6 meter	0.158	6.27	0.24	0.46	3.16E-04	0.022-0.31	376-5098	0.050-0.67	0-0.46	0-7557	0-1
Pitot Tube	0 m (smooth)	0.158	6.83	0.32	0.20	2.22E-04	-	-	-	0-0.20	0-4349	0-1
	1 meter	0.131	6.70	0.31	0.29	6.31E-05	-	-	-	0-0.29	0-6410	0-1
	3 meter	0.145	6.69	0.33	0.39	3.79E-05	-	-	-	0-0.39	0-9271	0-1
	6 meter	0.132	6.69	0.32	0.47	9.94E-05	-	-	-	0-0.47	0-10665	0-1

The power law exponents do not show a clear trend with increasing roughness as expected, but this is mostly due to the high exponents for the smooth wall data. If only considering the hot wire data with roughness elements, it can be seen that increasing roughness results in an increase in power law exponent. Similarly, the roughness heights calculated did not follow a clear trend except for the hot wire roughness data. For those three data sets, increased roughness elements resulted in an increased roughness length experienced by the flow, which is the expected result. However, the power law

exponents and roughness heights are on the right order of magnitude when compared to the previous Vincenti et al. data [6] and the ASCE data. The roughness heights are very small in magnitude compared to the ASCE roughness heights, but the boundary layer height in the experiments are also much smaller and the two are proportional. When both roughness heights are normalized by their boundary layer heights, the two are very similar.

The power law analysis fits the data well in the entire boundary layer, as expected. The spectral analysis, however, results in a much smaller region of agreement. However, as roughness is added, this region increases in size, which is the expected result and is the most promising result of this study. This region's increasing size will allow for more wind engineering applications to be available in the FPF. For example, taller buildings can be analyzed if the flow is comparable over a larger region.

Figure 12 below physically demonstrates the effects of the addition of roughness elements on the profile. The profile shifts upwards, meaning that the velocity gradient near the wall, and therefore the wall shear stress, is lessened. The boundary layer height varies for each profile, but they all approach similar freestream velocities. This result is expected because the FPF fans were run at 600RPM for all the experiments.
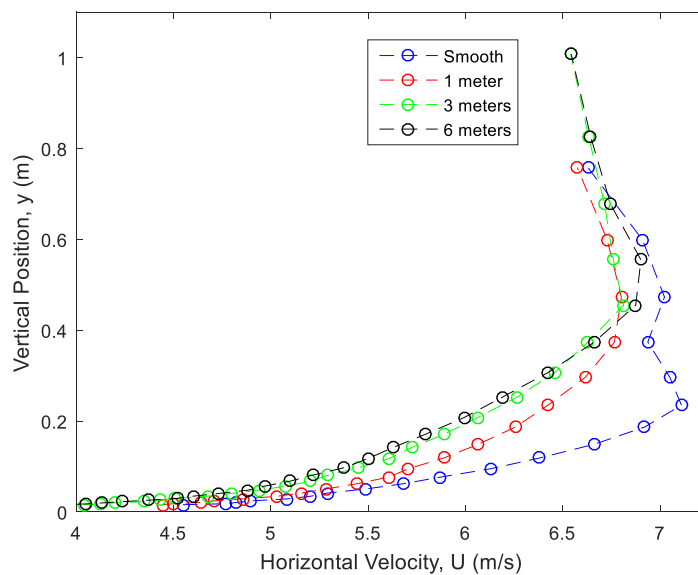
Figure 12: Position vs Velocity for Hot Wire Data collected in the FPF 16m downstream from inlet with the fans running at 600 RPM varying roughness lengths

VI. Conclusions

This project was the first step in re-creating several scaled-down ABLs in the FPF for wind engineering studies. The power law allowed for accurate fits to the mean profile data in the rough-wall

FPF boundary layer with reasonable power law exponents. The experimental power density spectra showed excellent agreement with the theoretical Von Karman spectra. Consistent with known ABL behaviors, the size of the regions where the power law and spectra agree increases with the addition of roughness elements. From our experiments, we conclude that the FPF wind tunnel can be configured to generate an accurate model of the ABL for wind engineering purposes. A final product of this project could be a scale model of a town, such as Durham, NH, for a wind analysis. To achieve this goal, we recommend that future studies explore a broader range of roughness conditions.

VII. References

[1] American Society of Civil Engineers (2012) Wind Tunnel Testing for Buildings and Other Structures: ASCE/SEI 49-12

[2] Counihan J (1971) Wind tunnel determination of the roughness length as a function of the fetch and the roughness density of three-dimensional roughness elements

[3] Fox, Robert W., Robert W. Fox, Philip J. Pritchard, and Alan T. McDonald. Fox and McDonald's Introduction to Fluid Mechanics. Hoboken, NJ: John Wiley & Sons, 2011. Print.

[4] Plate, E.J. (1971) Aerodynamic Characteristics of Atmospheric Boundary Layers. AEC Crit. Rev. Ser. TID-15465, Technical Information Center, US Department of Energy.

[5] Potier, Beth. "Media Relations." *Slow Flow: New Wind Tunnel Is Largest of Its Type*. UNH Media Relations, 15 Nov. 2010. Web

[6] Vincenti P; Klewicki J; Morrill-Winter C; White C; Wosnik M (2013) Streamwise Velocity Statistics in Turbulent Boundary Layers that Spatially Develop to High Reynolds Number

VII. Appendix

Table A.1: Properties required for ABL Simulation from ASCE 49-12 p.22 [1]

Class	Terrain Description	(z_o)[n] (m)	n[b]	$1/\alpha$[c]	f_c[d] (%)	^xL_o[n] (m)	Exposure[f]	z_g[f]
1	Open Sea, fetch at least 3 mi (5km)	~0.0002	0.10	0.09	9.2	190	D	213
2	Mud flats, snow; no vegetation, no obstacles	0.005	0.13		13.2	140	----	----
3	Open flat terrain; grass, few isolated obstacles	0.03	0.14	0.11	17.2	110	C	274
4	Low crops; occasional large obstacles, x'/h ~20	0.10	0.18		21.7	84	----	----
5	High crops; scattered obstacles, $15<x'/h<20$	0.25	0.22	0.14	27.1	64	B	366
6	Parkland, bushes: numerous obstacles, x'/h ~10	0.5	0.29		33.4	55	----	----
7	Regular large-obstacle coverage (suburb, forest)	1.0-2.0	0.33	0.20	43.4	45	A	457
8	City Center with high- and low-rise buildings	>2	0.40-0.67		----	----	----	----

Table A.2: Mean Velocity Profile Parameters from ASCE 49-12 p.3 [1]

| Exposure[n]	n	z_g(m)
D: Open Sea	.10	213
C: Open Flat Terrain	.14	274
B: High Crops, Scattered Obstacles	.22	366
A: Suburb, Forest	.33	457

Note: n is the power law exponent
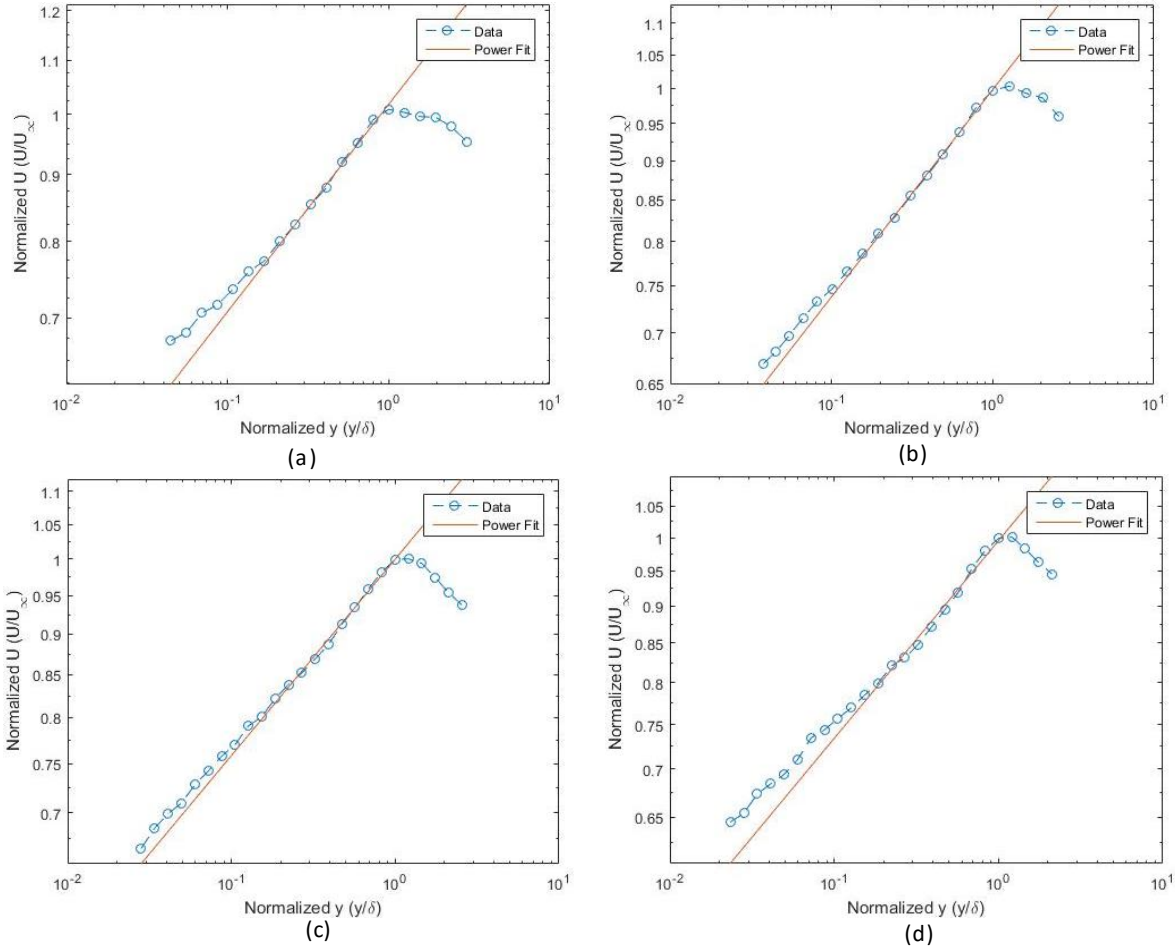
Figure A.1: Logarithmic plots of mean velocity profiles recorded with a pitot tube at 16m downstream of the FPF inlet with the fans running at 600 RPM with roughness array fetch lengths of (a) 0 meters (b) 1 meter (c) 3 meters (d) 6 meters
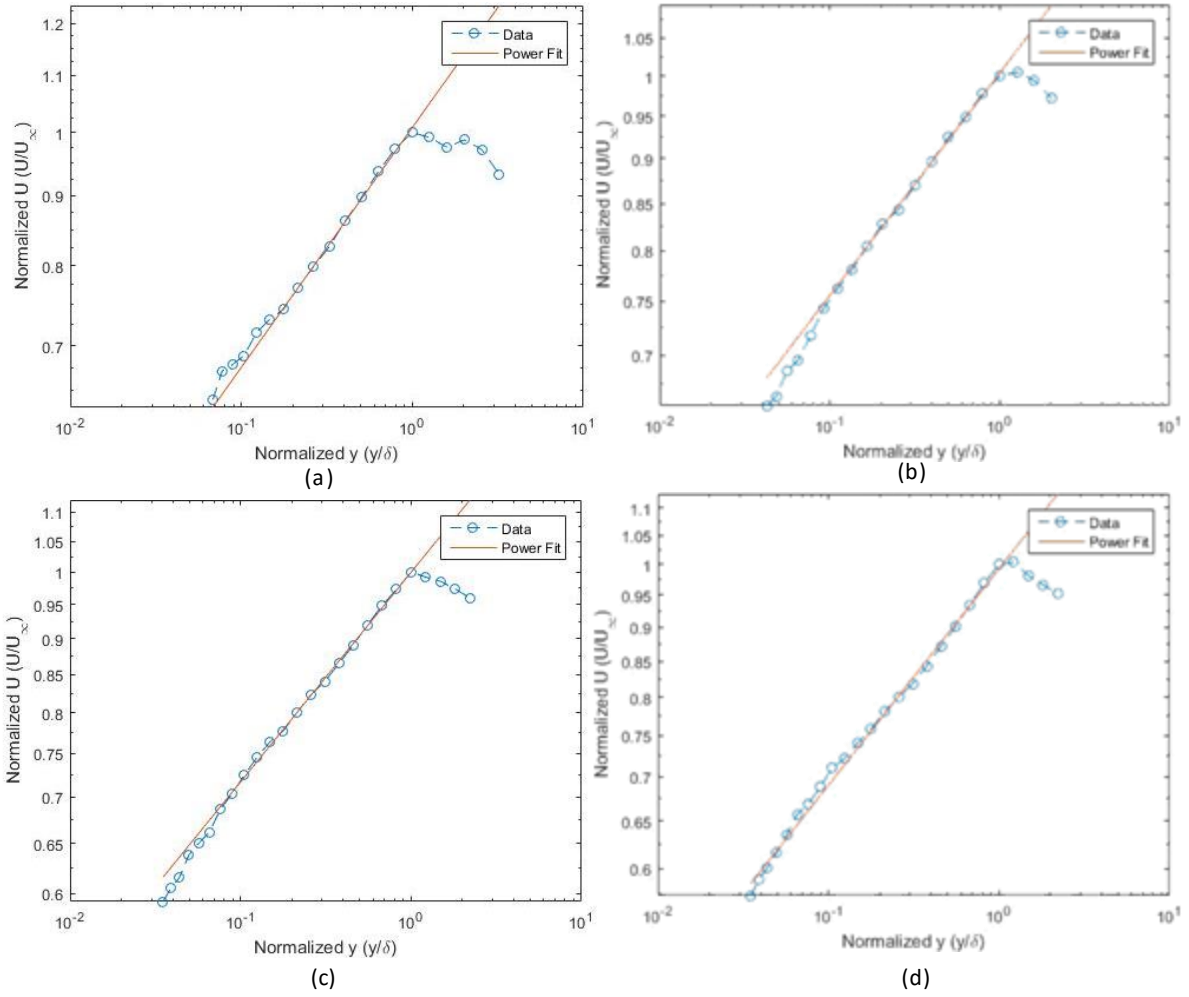
Figure A.2: Logarithmic plots of mean velocity profiles recorded with a hot wire anemometer at 16m downstream of the FPF inlet with the fans running at 600 RPM with roughness array fetch lengths of (a) 0 meters (b) 1 meter (c) 3 meters (d) 6 meters

Comments/Concerns for future senior project group:

Below is a figure of inner-normalized velocity and position for the hot wire data varying roughness. With additional roughness, the U+ vs y+ plots are expected to shift down, which is what happens except for the smooth wall data. Also, the smooth wall power exponent was much higher than the one we calculated using the VIncenti data at the same fan RPM and position downstream from the inlet of the tunnel. Maybe we just had faulty smooth wall data but these effects definitely need to be explored more.
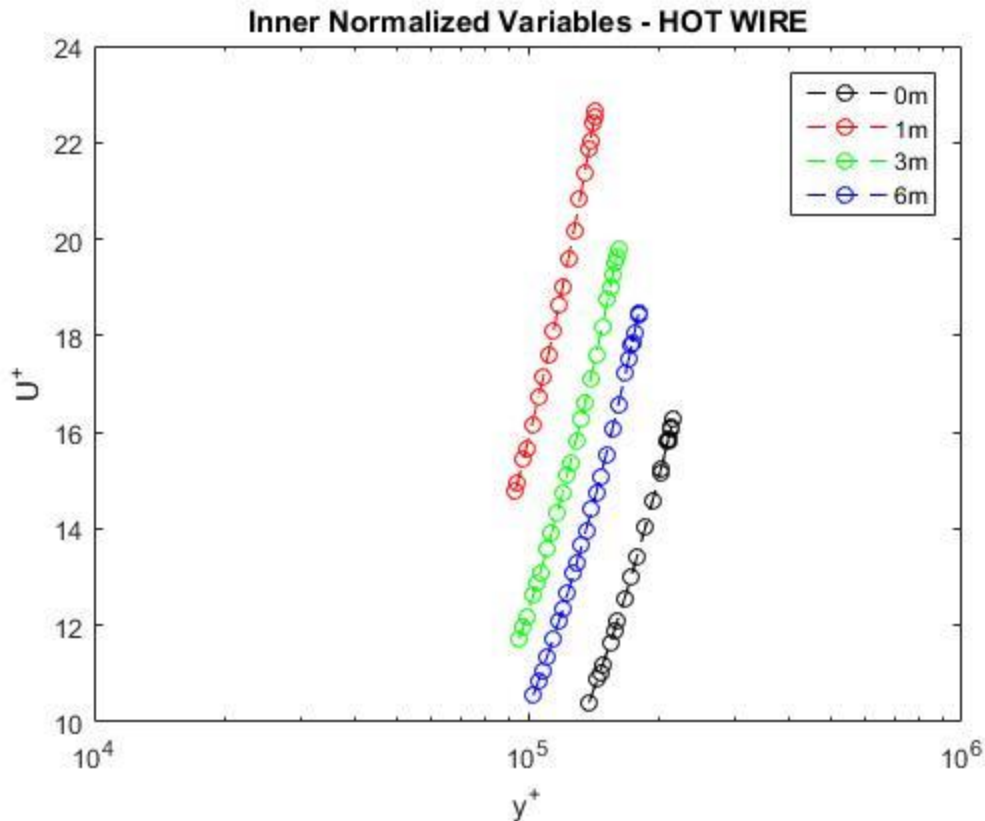
Also, the pitot tube data did not follow trends as clearly as the hot wire data, which is concerning. Again, perhaps the data needed to be collected on days with more similar weather patterns or something else went wrong during data collection, but this should be explored.